

Inhibitory Role of CD19 in the Progression of Experimental Autoimmune Encephalomyelitis by Regulating Cytokine Response

| | |
|------------------------------|---|
| 著者 | Matsushita Takashi, Fujimoto Manabu, Hasegawa Minoru, Komura Kazuhiro, Takehara Kazuhiko, Tedder Thomas F., Sato Shinichi |
| journal or publication title | American Journal of Pathology |
| volume | 168 |
| number | 3 |
| page range | 812-821 |
| year | 2006-03-01 |
| URL | http://hdl.handle.net/2297/45181 |

doi: 10.2353/ajpath.2006.050923

Inhibitory Role of CD19 in the Progression of Experimental Autoimmune Encephalomyelitis by Regulating Cytokine Response

Takashi Matsushita,* Manabu Fujimoto,* Minoru Hasegawa,* Kazuhiro Komura,*

Kazuhiko Takehara,* Thomas F. Tedder,[†] and Shinichi Sato*[‡]

From the Department of Dermatology,* Kanazawa University Graduate School of Medical Science, Kanazawa, Japan; the Department of Immunology,[†] Duke University Medical Center, Durham, NC, USA; and Department of Dermatology,[‡] Nagasaki University Graduate School of Biomedical Science, Nagasaki, Japan

Running head: Inhibitory Role of CD19 on EAE

Supported by the Ministry of Education, Science, and Culture of Japan, and the National Institutes of Health (grants CA105001, CA96547, and AI56363).

Address reprint requests to Manabu Fujimoto, MD, Department of Dermatology, Kanazawa University Graduate School of Medical Science, 13-1 Takaramachi, Kanazawa, Ishikawa 920-8641, Japan. E-mail: fujimoto-m@umin.ac.jp

Introduction

Lymphocytes accomplish a complex balance between proper response to foreign antigens and minimized reaction to self-antigens. Disruption of this balance can result in the induction of autoimmune diseases. Recent assessments of the role of B cells in the immune system have indicated that B cells have more essential functions in regulating immune responses than had previously been appreciated ¹⁻⁶. B cell functions include Ig secretion, antigen-presentation, production of various cytokines, and regulating lymphoid organogenesis, differentiation of T effector cells, and antigen-presenting dendritic cell function ⁷. Abnormalities of these B cell functions could contribute to the induction or development of autoimmunity. Thus, B cells are now considered as a potential therapeutic target in a wider range of autoimmune disorders ⁸. For example, B-cell depletion by anti-CD20 antibody (Ab) has shown unexpected impacts by dramatic effectiveness in treating patients with not only autoantibody-mediated diseases but also other various autoimmune disorders including rheumatoid arthritis ^{9,10}. On the other hand, recent studies have shown that B cells can also play a protective role against autoimmune diseases in certain circumstances ^{1,2}. Collectively, B cells have multiple critical roles in autoimmune disease expression through various functions.

Experimental autoimmune encephalomyelitis (EAE) is an inflammatory demyelinating disease of the central nerve system (CNS) that is primarily mediated by CD4⁺ T cells specific for CNS autoantigens, and is considered as a prototypic T helper type 1 (Th1)-mediated autoimmune disease ¹¹. Based on similarities in disease susceptibility, course, and histology, EAE is currently considered as an experimental animal model for multiple sclerosis in human, a common inflammatory and demyelinating disease of the CNS. Cytokines play a key role in the development and remission of EAE. The inflammatory lesion in the CNS requires a Th1 response, producing proinflammatory cytokines interferon- γ (IFN-

γ) and tumor necrosis factor- α (TNF- α)¹². Recovery is associated with production of Th2 cytokines, interleukin 4 (IL-4) and IL-10^{13,14}. Although EAE has long been considered as a T cell-mediated disease because adoptive transfer of neural antigen-specific T cells alone is sufficient to induce the disease¹⁵, recent studies have clarified roles of B cells and humoral immune response in the pathogenesis of EAE^{1,16-20}.

B cell fate and functions are largely determined by signal transduction through a B cell antigen receptor (BCR), which is further regulated by signal transduction molecules that amplify or inhibit BCR signaling during responses to self and foreign antigens. These regulatory molecules include a subset of functionally interrelated cell surface receptors, such as CD19, CD21, CD22, CD40, CD72, and Fc γ RIIb²¹. Especially, CD19 regulates basal signaling thresholds and accelerates BCR signal, and thus serves as a general 'rheostat' that defines signaling thresholds critical for B cell responses and autoimmunity²²⁻²⁴. Modulating CD19 expression and/or function has been shown to have great effects on normal immune responses and autoimmunity^{3,25-28}.

In the current study, we have assessed the roles of CD19 in EAE. Remarkably, CD19 expression influenced T cell differentiation and cytokine profile of the tissue. CD19 loss resulted in increased severity of the disease as well as delayed recovery, suggesting an inhibitory role of CD19 in the etiology of EAE.

Materials and Methods

Mice

CD19^{-/-} (C57BL/6 x 129) mice were generated as described²⁶ and backcrossed 12 generations onto the C57BL/6 background before use in this study. Wild type C57BL/6 mice were purchased from The Jackson Laboratory (Bar Harbor, Maine). Lack of cell-surface CD19 expression was verified by two-color immunofluorescence staining with flow cytometric

analysis. All mice were housed in a specific pathogen-free barrier facility and screened regularly for pathogens. All studies and procedures were approved by the Committee on Animal Experimentation of Kanazawa University Graduate School of Medical Science.

Peptide

MOG peptide (P35-55: MEVGWYRSPFSRVVHLYRNGK) was synthesized by Multiple Peptide Systems (San Diego, CA).

Induction and evaluation of EAE

Active EAE was induced in female mice (six- to eight-week-old) by subcutaneous immunization with 100 µg of MOG peptide emulsified in CFA containing 1 mg/ml of heat-killed *Mycobacterium tuberculosis* H37RA (Sigma-Aldrich, St. Louis, MO) on days 0 and 7. Additionally, mice received 200 ng of pertussis toxin (Sigma-Aldrich) intraperitoneally in 0.5 ml of PBS on days 0 and 2. Clinical signs of EAE were assessed daily with a 0-6 scoring system (0, no signs; 1, flaccid tail; 2, impaired righting reflex and/or gait; 3, partial hind limb paralysis; 4, total hind limb paralysis; 5, hind limb paralysis with partial fore limb paralysis; 6, moribund or dead). Differences in total disease burdens between groups were analyzed with Mann-Whitney U test.

Serological evaluation of MOG peptide-specific Ig production

Serum was obtained 14 and 28 days after immunization. ELISA was used for detection of MOG peptide-specific Ab. Briefly, 96 well microtiter plates (Costar, Cambridge, MA) were coated with 10 µg/ml of MOG peptide. Plates were incubated with serum samples diluted 1:100. The bound Abs were detected with alkaline phosphatase-conjugated goat anti-mouse IgG or goat anti-mouse IgM Abs (Southern Biotechnology Associates, Inc., Birmingham, AL).

Histology

MOG-induced EAE mice were euthanized on day 28 and perfused by intracardiac injection of 4% paraformaldehyde and 1% glutaraldehyde in PBS. Transverse sections of the cervical, upper thoracic, lower thoracic, and lumbar region of the spinal cord were stained with H&E or Luxol Fast Blue-Periodic acid. Each spinal cord section was further subdivided into an anterior, posterior, and two lateral columns. Each subdivided area displaying either lymphocyte infiltration or demyelination was assigned a score of one; thus, each animal had a potential maximum score of 16.

For immunohistochemistry, frozen tissue sections of the spinal cord were acetone fixed and then incubated with 10% normal rabbit serum in PBS (10 min, 37°C) to block nonspecific staining. Sections were then incubated with rat mAbs specific for mouse macrophages (F4/80), CD4 (Clone RM4-5; BD PharMingen, San Diego, CA), and CD8 (clone 53-6.7; BD PharMingen). Rat IgG (Southern Biotechnology Associates, Inc.) was used as a control for nonspecific staining. Sections were then incubated sequentially (20 min, 37°C) with a biotinylated rabbit anti-rat IgG and then HRP-conjugated avidin-biotin complexes (Vectastain ABC kit; Vector Laboratories, Burlingame, CA). Sections were developed with 3,3'-diaminobenzidine tetrahydrochloride and hydrogen peroxide and then counterstained with methyl green.

Isolation of total RNA and real-time RT-PCR

After perfusion with PBS, spinal cord from each MOG-induced EAE mouse was collected. Total RNA from spinal cord was extracted using QIAGEN RNeasy spin columns (QIAGEN Ltd., Crawley, UK) and digested DNase I (QIAGEN Ltd.) to remove chromosomal DNA in accordance with the manufacture's protocol. Total RNA was reverse transcribed to cDNA

using Reverse Transcription System with random hexamers (Promega, Madison, WI). Real-time quantitative RT-PCR was performed using the TaqMan® system (Applied Biosystems, Foster City, CA) on ABI Prism 7000 Sequence Detector (Applied Biosystems) according to the manufacture's instructions. TaqMan® probes and primers for IFN- γ , IL-12p40, TNF- α , IL-6, IL-10, and glyceraldehyde-3-phosphate dehydrogenase (GAPDH) were purchased from Applied Biosystems. Relative expression of real-time PCR products was determined using the $\Delta\Delta C_T$ technique²⁹. Briefly, each set of samples was normalized using the difference in threshold cycle (C_T) between the target gene and housekeeping gene (GAPDH): $\Delta C_T = (C_{T \text{ target gene}} - C_{T \text{ GAPDH}})$. Relative mRNA levels were calculated by the expression $2^{-\Delta\Delta C_T}$ where $\Delta\Delta C_T = \Delta C_{T \text{ sample}} - \Delta C_{T \text{ calibrator}}$. Each reaction was done in, at least, triplicate.

Isolation of mononuclear cells from the CNS and Flow cytometric analysis

After perfusion with PBS, cells from the CNS were isolated as previously described³⁰. Briefly, tissues were dissociated by passing through 100- μ m cell strainer, then centrifuged at 400 $\times g$ for 10 min at 4°C. The pellet was resuspended in 70% isotonic Percoll (Pharmacia, Piscataway, NJ), overlaid with equal volumes of 37 and 30% isotonic Percoll, and centrifuged at 500 $\times g$ for 20 min at room temperature. Cells were collected from the 37:70% interface and washed.

For intracellular IFN- γ staining, collected cells were stimulated for 4 h at 37°C with 25 ng/ml PMA (Sigma-Aldrich) and 1 μ g/ml ionomycin (Sigma-Aldrich) in 1 ml of complete medium containing the intracellular transport inhibitor brefeldin A (10 μ g/ml; Sigma-Aldrich). The cells were stained with anti-CD4 (RM4-5; BD PharMingen) and anti-CD8 (53-6.7; BD PharMingen) Abs, and then washed and treated with FACS permeabilizing solution (BD Biosciences, San Jose, CA) for 10 min at room temperature. These cells were incubated

for 30 min in the dark with anti-IFN- γ Ab (XMG1.2; BD Biosciences). The Cells were analyzed on a FACScan flow cytometer (BD Biosciences).

Production of IL-10 and IFN- γ by splenic B cells

Splenic B cells from MOG-induced EAE on day 28 were purified (>95% B220⁺) by removing T cells with anti-Thy1.2 Ab-coated magnetic beads (DynaL Inc. Lake Success, NY). Purified splenic B cells were cultured in RPMI 1640 containing 10% heat-inactivated FCS, 100 U/ml penicillin, and 100 μ g/ml streptomycin, 2×10^{-5} M β -mercaptoethanol, and 2 mM L-glutamine (Gibco, Life Technologies, Paisley, UK). B cells were cultured in 96-well flat-bottom plates (Becton Dickinson, Franklin Lakes, NJ) at 4×10^5 cells per well with 40 μ g/ml of MOG peptide and 10 μ g/ml of anti-CD40 mAb (1C10; R&D systems, Minneapolis, MN) for 5 days. Control cultures were stimulated with MOG alone or anti-CD40 mAb alone. Each sample was done in triplicate. IL-10 and IFN- γ accumulation in the culture medium was measured by ELISA according to the manufacturer's protocol (R&D systems).

For intracellular IL-10 and IFN- γ staining, purified splenic B cells were stimulated at 1×10^6 cells/ml with 40 μ g/ml of MOG peptide and 10 μ g/ml of anti-CD40 mAb for 72 h, and then restimulated with 25 ng/ml PMA and 1 μ g/ml ionomycin for 12 h. Brefeldin A (10 μ g/ml) was added 8 h after the cultures were initiated. The cells were stained with anti-B220 (RA3-6B2; BD PharMingen) Abs, and then washed and treated with FACS permeabilizing solution for 10 min at room temperature. These cells were incubated for 30 min in the dark with anti-IL-10 (JES5-16E3; BD Biosciences) and anti-IFN- γ Abs. The Cells were analyzed on a FACScan flow cytometer (BD Biosciences).

Adoptive transfer of MOG-primed B cells

CD19^{-/-} and wild type mice were immunized with MOG peptide to induce EAE. MOG-primed splenic B cells were collected from MOG-induced EAE on day 28 and purified (>95% B220⁺) by removing T cells with anti-Thy1.2 Ab-coated magnetic beads (DynaL Inc.). Then 10⁷ B cells from CD19^{-/-} and wild type mice were transferred intravenously into wild type and CD19^{-/-} mice, respectively. One day later, the recipient mice were immunized with MOG peptide to induce EAE.

Statistical analysis

All data are expressed as the mean value ± SEM. Mann-Whitney U-test was used for determining the level of significance of differences between sample means.

Results

Increased severity of EAE in CD19^{-/-} mice

To assess whether CD19 expression plays a role in the pathogenesis of EAE, we immunized CD19^{-/-} mice and wild type C57BL/6 mice with myelin oligodendrocyte glycoprotein (MOG) peptide in complete Freund's adjuvant (CFA), and the course of the clinical disease was observed. In both lines of mice, EAE was induced at days 12-14, with a peak at days 18-23, followed by the plateau phase (Figure 1). However, compared with wild type mice, CD19^{-/-} mice showed significantly higher score at the peak and the plateau phase. Thus, CD19^{-/-} mice were more susceptible to EAE. This was consistent with histological findings of the inflamed CNS tissue, which revealed that CD19^{-/-} mice developed more severe inflammation (Figure 2A). To further evaluate the pathologic severity, transverse sections of the cervical, upper thoracic, lower thoracic, and lumbar region of the spinal cord were stained with H&E and Luxol Fast Blue-Periodic acid, and scored for the degree of inflammation and demyelination. Areas of inflammation and demyelination were more widespread in CD19^{-/-} mice when

compared with those in wild type mice at day 28 (Figure 2E). The pathologic scores in the CD19^{-/-} mice were significantly higher with 11.4 ± 1.1 for inflammation and 7.4 ± 1.8 for demyelination, while in the wild type mice, the scores for inflammation and demyelination were 5.2 ± 0.7 and 2.8 ± 0.5 , respectively ($p < 0.005$ and $p < 0.05$, respectively; Figure 2E). Collectively, CD19^{-/-} mice developed more severe EAE both clinically and pathologically than wild type mice.

CD8⁺ T cells were selectively increased in the inflamed CNS from CD19^{-/-} mice with EAE

To further evaluate the pathology of EAE in CD19^{-/-} mice, the infiltrating cells in the inflamed CNS were examined by immunostaining. As shown in Table 1, the frequency of infiltrating CD4⁺ T cells was not significantly different between CD19^{-/-} and wild type mice, while the frequency of CD8⁺ T cells was significantly 1.9-fold higher in CD19^{-/-} mice than in wild type mice. The representative photomicrographs of CNS-infiltrating CD4⁺ and CD8⁺ T cells were shown in Figure 2C and 2D. The ratio of CD4/CD8 T cells in CD19^{-/-} mice was 1.4 ± 0.5 , significantly lower than that found in wild type mice (3.3 ± 1.5). CD4/CD8 T cell ratio was not altered in the peripheral blood in CD19^{-/-} mice with or without EAE when compared with wild type mice (data not shown). Additionally, the number and percentage of macrophages were not different between the two groups (Table 1). Also, B cell infiltration was not found in either line of mice (data not shown). CD19 expression was not detected in infiltrating T lymphocytes or macrophages (data not shown). Thus, CD8⁺ T cells were selectively increased in the inflamed CNS from CD19^{-/-} mice with EAE.

CD19 loss attenuated anti-MOG Ig production in MOG-induced EAE

To dissect the mechanism by which CD19-deficiency enhanced the disease severity, serum IgM and IgG anti-MOG Ab levels were measured by ELISA. Sera were collected from CD19^{-/-} and wild type mice with EAE on days 14 and 28. Serum IgM anti-MOG Abs levels in wild type mice with EAE were significantly increased compared to control mice immunized with CFA alone 28 days after immunization ($p < 0.005$; Figure 3A). Additionally, serum IgG anti-MOG Abs levels in wild type mice with EAE were significantly elevated compared to normal controls 14 and 28 days after immunization ($p < 0.005$ and $p < 0.005$, respectively; Figure 3B). By contrast, the serum levels of IgM and IgG anti-MOG Abs stayed significantly lower in CD19^{-/-} mice with EAE, which showed no significantly higher levels than wild type mice without MOG immunization (Figure 3). Thus, the loss of CD19 expression dramatically inhibited anti-MOG Ab production in EAE.

To test whether decreased anti-MOG Ab enhanced the disease severity in CD19^{-/-} mice, sera from wild type mice with EAE were transferred to CD19^{-/-} mice with EAE. However, no alteration of disease course was observed in CD19^{-/-} mice that received sera from wild type mice with EAE (data not shown), suggesting that decreased anti-MOG Ab is not solely responsible for the increased severity of EAE in CD19^{-/-} mice.

The inflamed CNS tissue in CD19^{-/-} mice displays a Th1 bias

To assess the cytokine expression profile of CNS-infiltrating cells, spinal cords were harvested from wild type mice and CD19^{-/-} mice 28 days after MOG immunization, and cytokine expression was analyzed by real-time PCR (Figure 4A). The mRNA expressions of Th1 cytokines, IFN- γ and IL-12p40, in CD19^{-/-} mice were increased compared with wild type mice (2.5-fold; $p < 0.05$ and 2.0-fold, respectively). The mRNA expression of TNF- α , a proinflammatory cytokine, in CD19^{-/-} mice was also slightly higher by 1.5-fold than wild type mice. IL-6 mRNA expression in CD19^{-/-} mice was comparable to wild type mice. By contrast,

spinal cords from CD19^{-/-} mice showed dramatically decreased mRNA expressions of IL-10, a Th2 cytokine, compared with wild type mice (77% decrease, p<0.05; Figure 4A). To address what cell types may be accounting for excess of IFN- γ in the CNS of CD19^{-/-} mice when compared to wild type mice, flow cytometric intracellular cytokine staining was performed. IFN- γ production from CNS infiltrating CD4⁺ T cells in CD19^{-/-} mice was augmented compared to wild type (Figure 4B). In addition, IFN- γ production from CD8⁺ T cells in CD19^{-/-} mice was also augmented (Figure 4C). Thus, it was likely that excess of IFN- γ in the CNS of CD19^{-/-} mice were generated by CD4⁺ and CD8⁺ T cell collaboration. These findings indicate that the inflamed CNS tissue of CD19^{-/-} mice with EAE displays a Th1 bias and that this skewed cytokine balance may contribute to the augmented disease manifestation.

CD19 deficiency suppressed IL-10 production from B cells

Since a recent study has demonstrated that IL-10 from B cells is important for EAE recovery ¹, we next investigated the difference of IL-10 production in B cells from CD19^{-/-} mice and wild type mice. Splenic B cells were purified from CD19^{-/-} mice and wild type mice at day 28, followed by in vitro stimulation. Incubation with MOG alone resulted in modest and comparable IL-10 production both in CD19^{-/-} and wild type B cells (Figure 5A). By contrast, an agonistic Ab to CD40 induced higher levels of IL-10 production in wild type B cells than in CD19^{-/-} B cells (Figure 5A). Concomitant stimulation with MOG and anti-CD40 Ab further increased IL-10 production in wild type B cells, while it did not increase IL-10 production in CD19^{-/-} B cells. In addition, IL-10 production from B cells was confirmed using intracellular cytokine staining. Wild type B cells produced IL-10 with MOG and anti-CD40 Ab stimulations, whereas CD19^{-/-} B cells did not (Figure 5B). Thus, anti-CD40-induced IL-10 production was impaired in CD19^{-/-} B cells with or without antigen stimulation.

CD19 deficiency increased IFN- γ production from B cells

We also examined in vitro B cell production of IFN- γ using purified splenic B cells from CD19^{-/-} and wild type mice 28 days after immunization. B cells from wild type or CD19^{-/-} mice incubated with MOG alone did not produce IFN- γ (Figure 5B). Anti-CD40 Ab induced only slight increase of IFN- γ production, if any, in wild type B cells, while B cells from CD19^{-/-} mice demonstrated increased IFN- γ production against anti-CD40 Ab (Figure 5B). Furthermore, addition of MOG to anti-CD40 Ab greatly increased IFN- γ production in CD19^{-/-} B cells, while wild type B cells showed only modest IFN- γ production by MOG and anti-CD40 Ab stimulation (Figure 5B). In addition, IFN- γ production from B cells was confirmed using intracellular cytokine staining. IFN- γ production from CD19^{-/-} B cells with MOG and anti-CD40 Ab stimulations was augmented compared to wild type B cells (Figure 5C). Unlike IFN- γ , B cells from CD19^{-/-} and wild type mice with MOG and anti-CD40 Ab stimulation produced scant but comparable amount of IL-12, another Th1 cytokine (data not shown). Therefore, anti-CD40-induced IFN- γ production was augmented in CD19^{-/-} B cells, which was further exaggerated by the presence of antigen. Collectively, CD19^{-/-} B cells showed skewed cytokine response with increased IFN- γ production and decreased IL-10 production.

Adoptive transfer of CD19^{-/-} B cells increased the severity of EAE in wild type mice

We next assessed whether the altered B cell functions, especially cytokine production, were responsible in vivo for increased severity of EAE in CD19^{-/-} mice. First, MOG-primed B cells (10^7 cells, >95% B220⁺) by removing T cells with anti-Thy1.2 Ab from wild type mice with EAE were adoptively transferred to CD19^{-/-} mice prior to EAE induction. However, CD19^{-/-} mice which received wild type B cells developed EAE with almost the same severity as

CD19^{-/-} mice receiving no B cells (Figure 6A). Therefore, the failure of IL-10 production from B cells alone did not explain the increased severity of EAE in CD19^{-/-} mice. Next, MOG-primed B cells (10⁷ cells, >95% B220⁺) from CD19^{-/-} mice with EAE were adoptively transferred to wild type mice prior to EAE induction. Wild type mice which received CD19^{-/-} B cells developed EAE with significantly higher severity than wild type mice receiving no B cells and exhibited as severe EAE as CD19^{-/-} mice (Figure 6B). To exclude dendritic cells or NK cells contaminations in adoptive transfer of B cells, we yielded high purity B cells (>99% B220⁺) by removing T cells, NK cells, monocytes, macrophages, dendritic cells, granulocytes and erythrocytes with antibodies for mouse CD43, CD4 and Ter-119. The results of adoptive transfer of B cells using high purity B cells (>99% B220⁺) were comparable to using conventional purity B cells (>95% B220⁺) by removing T cells with anti-Thy1.2 Ab (data not shown). Thus, exaggerated B cell functions, especially excessive IFN- γ production from B cells, may increase severity of EAE in CD19^{-/-} mice.

Discussion

In the current study, we assessed the role of CD19, a B cell-specific cell-surface molecule, in the induction and recovery of EAE. CD19 loss resulted in both increased severity and prolonged recovery of the disease (Figure 1). This result was striking since CD19^{-/-} mice generally exhibit an immunodeficient phenotype^{25,26,28}. CD19^{-/-} mice with EAE showed increased CD8⁺ T cell infiltration but not increased CD4⁺ T cell infiltration in the inflamed CNS (Table 1, Figure 2C and 2D). Furthermore, cytokine expression profile was shifted to Th1 in the CNS from CD19^{-/-} mice when compared with wild type mice (Figure 4). CD19^{-/-} mice with EAE also showed decreased serum IgM and IgG anti-MOG Abs (Figure 3), although serum transfer between CD19^{-/-} and wild type mice did not alter disease severity. Remarkably, adoptive transfer of B cells from CD19^{-/-} mice with EAE to wild type mice

enhanced the disease severity in the recipient wild type mice (Figure 6). By contrast, wild type B cells did not rescue EAE in CD19^{-/-} mice. Therefore, the loss of a single B cell-specific protein, CD19, was sufficient to modify the disease manifestation of EAE, suggesting inhibitory role of CD19 in the etiology of the disease.

While there are some discrepancies among studies, the importance of B cells in EAE has been reported, although the mechanisms are still controversial. Mice genetically deficient for B cells develop EAE^{16,31}, but fail to resolve the disease^{1,16}. Therefore, B cells or Ab are not required for primary induction of EAE, while antigen-specific B cells are essential for the recovery from the disease. Fillatreau et al. have demonstrated that IL-10 production from B cells plays a key role in resolving EAE, suggesting a regulatory role of B cells in the disease. Furthermore, another study using mice deficient for Lyn, a Src-family protein tyrosine kinase expressed abundantly in B cells, has demonstrated that Lyn-deficient (Lyn^{-/-}) mice show both increased severity and more sustained course of EAE and that serum transfer from Lyn^{-/-} mice worsens EAE in wild type mice¹⁸. The current study has shown that the loss of CD19 expression increased severity of EAE at the peak and the plateau phase. Taken together, B cells appear to have multiple roles during the process of EAE.

CD19 positively regulates B cell response to a variety of transmembrane signals^{23,24}. B cells from CD19^{-/-} mice are hyporesponsive to antigen, anti-CD40, LPS, and other stimuli^{25,26,28}. Consistent with this, CD19^{-/-} mice immunized with MOG peptide produced lower levels of IgM and IgG anti-MOG Ab than wild type mice. CD19 regulates B cell signaling pathways by acting as a scaffold protein that recruits Lyn, PI 3-kinase, Vav, and possibly other molecules²². CD19^{-/-} mice and Lyn^{-/-} mice both show increased severity of EAE¹⁸. CD19 regulates Lyn kinase activity in BCR signaling²², although the mechanisms exaggerating EAE appear different between the two lines of mice since augmented Ab response appears the main mechanism in Lyn^{-/-} mice. In the case of CD19^{-/-} mice, serum

transfer did not alter the disease severity. Additionally, mRNA levels of IFN- γ are decreased in the inflamed CNS from Lyn^{-/-} mice. By contrast, B cells from CD19^{-/-} mice with EAE produced significantly higher levels of IFN- γ in response to MOG and anti-CD40 Ab than wild type mice, while MOG and anti-CD40 Ab induced less IL-10 production in B cells from CD19^{-/-} mice with EAE than those from wild type mice with EAE. Thus, CD19 regulates IL-10 production positively and IFN- γ negatively, and this shifted balance likely affected the disease severity of EAE. The mechanism by which CD19 regulates cytokine production is still unclear. Since CD19 has been shown to regulate BCR-induced STAT1 phosphorylation³² which has a critical role in IFN-induced response, altered STAT1 function by CD19 loss may affect the signaling pathway. CD19 may also regulate other cytokine signaling such as JAK/STAT. Therefore, CD19 may directly regulate IL-10 and/or IFN- γ production pathway(s). Alternatively, CD19 regulation on the signal strength to stimuli may indirectly affect the cytokine balance. In either manner, CD19 can control Th1/Th2 cytokine balance in B cells by the reciprocal regulation between IFN- γ and IL-10.

The adoptive transfer experiments have demonstrated that wild type B cells did not rescue EAE in CD19^{-/-} mice but that CD19^{-/-} B cells worsened EAE in wild type mice. Therefore, B cells deficient for CD19 have a positive role for driving the disease. The most likely explanation for this phenomenon is excessive production of IFN- γ by CD19^{-/-} B cells. Recent studies have emphasized B cells as an important source of IFN- γ ³³⁻⁴⁰. IFN- γ production in B cells is induced by IL-12^{35,37-40}, while B cells downregulate Th1 response via the release of IL-10^{1,2}. Additionally, the autoreactive B cells function as highly efficient antigen presenting cells, enhancing the selective action of MOG-specific T cells⁴¹. B cell-T cell interaction with B cell antigen presentation favors Th2, rather than Th1, differentiation^{42,43}. Therefore, excessive production of IFN- γ from CD19^{-/-} B cells can negatively regulate B

cell antigen presentation, and then can commit T cells to Th1 phenotype. Intriguingly, the inflamed CNS of CD19^{-/-} mice exhibited an increase in TNF- α and Th1 cytokines such as IFN- γ and IL-12p40 and a decrease in Th2 cytokine such as IL-10, although there was no B cell infiltration. Thus, skewed cytokine production of B cells influenced the total cytokine profile in the tissue.

Another striking finding in the current study was a specific increase of CD8⁺ T cells in spinal cord of CD19^{-/-} mice. EAE is considered to be CD4⁺ T cell-driven¹⁵, associated with inflammatory cytokine profile. However, recent studies have shown that CD8⁺ T cells have a disease-promoting role⁴⁴. Furthermore, it has been demonstrated that T cells infiltrating into active human MS lesions are dominated by CD8⁺ T cells⁴⁵. Thus, the increase in CD8⁺ T cells in inflamed CNS of CD19^{-/-} mice may have relevance with more severe EAE.

Previous studies have shown that MOG-specific antibodies enhance demyelination and inflammation, resulting in increased severity of EAE^{19,20}. Furthermore, plasma exchange can reduce clinical disease activity in a subset of MS patients^{46,47}; therefore, humoral factors play an important role in MS and EAE. However, MOG-specific antibodies had no direct effect on EAE induction in the current study. Although the reasons for this discrepancy are not clear, B cell functions for cytokine producing and antigen presenting cells may be more important than MOG-specific antibody productions in the current study. It is possible that CD19^{-/-} B cells act as antigen presenting cells and stimulate autoantigen-specific CD8⁺ T cells, contributing to exacerbation of EAE.

In conclusion, the current study has shown that CD19 plays an important role in the development of EAE. CD19 is a critical factor for T cell commitment to the Th2 phenotype. Thus, modulating CD19 function or its pathway may be a potential therapeutic target of MS and other Th1 diseases.

Acknowledgments

We thank Ms M. Matsubara and Y. Yamada for technical assistance.

References

1. Fillatreau S, Sweenie CH, McGeachy MJ, Gray D, Anderton SM: B cells regulate autoimmunity by provision of IL-10. *Nat Immunol* 2002, 3:944-950
2. Mauri C, Gray D, Mushtaq N, Londei M: Prevention of arthritis by interleukin 10-producing B cells. *J Exp Med* 2003, 197:489-501
3. Saito E, Fujimoto M, Hasegawa M, Komura K, Hamaguchi Y, Kaburagi Y, Nagaoka T, Takehara K, Tedder TF, Sato S: CD19-dependent B lymphocyte signaling thresholds influence skin fibrosis and autoimmunity in the tight-skin mouse. *J Clin Invest* 2002, 109:1453-1462
4. Weinstein E, Peeva E, Putterman C, Diamond B: B-cell biology. *Rheum Dis Clin North Am* 2004, 30:159-174
5. Chan OT, Madaio MP, Shlomchik MJ: B cells are required for lupus nephritis in the polygenic, Fas-intact MRL model of systemic autoimmunity. *J Immunol* 1999, 163:3592-3596
6. Ji H, Ohmura K, Mahmood U, Lee DM, Hofhuis FM, Boackle SA, Takahashi K, Holers VM, Walport M, Gerard C, Ezekowitz A, Carroll MC, Brenner M, Weissleder R, Verbeek JS, Duchatelle V, Degott C, Benoist C, Mathis D: Arthritis critically dependent on innate immune system players. *Immunity* 2002, 16:157-168
7. Lipsky PE: Systemic lupus erythematosus: an autoimmune disease of B cell hyperactivity. *Nat Immunol* 2001, 2:764-766
8. Martin F, Chan AC: Pathogenic roles of B cells in human autoimmunity; insights from the clinic. *Immunity* 2004, 20:517-527
9. Edwards JC, Szczepanski L, Szechinski J, Filipowicz-Sosnowska A, Emery P, Close DR, Stevens RM, Shaw T: Efficacy of B-cell-targeted therapy with rituximab in patients with rheumatoid arthritis. *N Engl J Med* 2004, 350:2572-2581

10. Shaw T, Quan J, Totoritis MC: B cell therapy for rheumatoid arthritis: the rituximab (anti-CD20) experience. *Ann Rheum Dis* 2003, 62 Suppl 2:ii55-59
11. Williams KC, Ulvestad E, Hickey WF: Immunology of multiple sclerosis. *Clin Neurosci* 1994, 2:229-245
12. Kuchroo VK, Martin CA, Greer JM, Ju ST, Sobel RA, Dorf ME: Cytokines and adhesion molecules contribute to the ability of myelin proteolipid protein-specific T cell clones to mediate experimental allergic encephalomyelitis. *J Immunol* 1993, 151:4371-4382
13. Khoury SJ, Hancock WW, Weiner HL: Oral tolerance to myelin basic protein and natural recovery from experimental autoimmune encephalomyelitis are associated with downregulation of inflammatory cytokines and differential upregulation of transforming growth factor beta, interleukin 4, and prostaglandin E expression in the brain. *J Exp Med* 1992, 176:1355-1364
14. Kennedy MK, Torrance DS, Picha KS, Mohler KM: Analysis of cytokine mRNA expression in the central nervous system of mice with experimental autoimmune encephalomyelitis reveals that IL-10 mRNA expression correlates with recovery. *J Immunol* 1992, 149:2496-2505
15. Pettinelli CB, McFarlin DE: Adoptive transfer of experimental allergic encephalomyelitis in SJL/J mice after in vitro activation of lymph node cells by myelin basic protein: requirement for Lyt 1+ 2- T lymphocytes. *J Immunol* 1981, 127:1420-1423
16. Wolf SD, Dittel BN, Hardardottir F, Janeway CA, Jr.: Experimental autoimmune encephalomyelitis induction in genetically B cell-deficient mice. *J Exp Med* 1996, 184:2271-2278
17. Cross AH, Trotter JL, Lyons J: B cells and antibodies in CNS demyelinating disease. *J Neuroimmunol* 2001, 112:1-14

18. Du C, Sriram S: Increased severity of experimental allergic encephalomyelitis in lyn^{-/-} mice in the absence of elevated proinflammatory cytokine response in the central nervous system. *J Immunol* 2002, 168:3105-3112
19. Linington C, Bradl M, Lassmann H, Brunner C, Vass K: Augmentation of demyelination in rat acute allergic encephalomyelitis by circulating mouse monoclonal antibodies directed against a myelin/oligodendrocyte glycoprotein. *Am J Pathol* 1988, 130:443-454
20. Lyons JA, San M, Happ MP, Cross AH: B cells are critical to induction of experimental allergic encephalomyelitis by protein but not by a short encephalitogenic peptide. *Eur J Immunol* 1999, 29:3432-3439
21. Tsubata T: Co-receptors on B lymphocytes. *Curr Opin Immunol* 1999, 11:249-255
22. Fujimoto M, Fujimoto Y, Poe JC, Jansen PJ, Lowell CA, DeFranco AL, Tedder TF: CD19 regulates Src family protein tyrosine kinase activation in B lymphocytes through processive amplification. *Immunity* 2000, 13:47-57
23. Tedder TF, Poe JC, Fujimoto M, Haas KM, Sato S: The CD19-CD21 signal transduction complex of B lymphocytes regulates the balance between health and autoimmune disease: systemic sclerosis as a model system. *Curr Dir Autoimmun* 2005, 8:55-90
24. Fujimoto M, Poe JC, Hasegawa M, Tedder TF: CD19 regulates intrinsic B lymphocyte signal transduction and activation through a novel mechanism of processive amplification. *Immunol Res* 2000, 22:281-298
25. Rickert RC, Rajewsky K, Roes J: Impairment of T-cell-dependent B-cell responses and B-1 cell development in CD19-deficient mice. *Nature* 1995, 376:352-355

26. Engel P, Zhou LJ, Ord DC, Sato S, Koller B, Tedder TF: Abnormal B lymphocyte development, activation, and differentiation in mice that lack or overexpress the CD19 signal transduction molecule. *Immunity* 1995, 3:39-50
27. Asano N, Fujimoto M, Yazawa N, Shirasawa S, Hasegawa M, Okochi H, Tamaki K, Tedder TF, Sato S: B Lymphocyte signaling established by the CD19/CD22 loop regulates autoimmunity in the tight-skin mouse. *Am J Pathol* 2004, 165:641-650
28. Sato S, Steeber DA, Tedder TF: The CD19 signal transduction molecule is a response regulator of B-lymphocyte differentiation. *Proc Natl Acad Sci U S A* 1995, 92:11558-11562
29. Bloch G, Toma DP, Robinson GE: Behavioral rhythmicity, age, division of labor and period expression in the honey bee brain. *J Biol Rhythms* 2001, 16:444-456
30. Zeine R, Owens T: Direct demonstration of the infiltration of murine central nervous system by Pgp-1/CD44^{high} CD45RB^(low) CD4⁺ T cells that induce experimental allergic encephalomyelitis. *J Neuroimmunol* 1992, 40:57-69
31. Hjelmstrom P, Juedes AE, Fjell J, Ruddle NH: B-cell-deficient mice develop experimental allergic encephalomyelitis with demyelination after myelin oligodendrocyte glycoprotein sensitization. *J Immunol* 1998, 161:4480-4483
32. Su L, Rickert RC, David M: Rapid STAT phosphorylation via the B cell receptor. Modulatory role of CD19. *J Biol Chem* 1999, 274:31770-31774
33. Pang Y, Norihisa Y, Benjamin D, Kantor RR, Young HA: Interferon-gamma gene expression in human B-cell lines: induction by interleukin-2, protein kinase C activators, and possible effect of hypomethylation on gene regulation. *Blood* 1992, 80:724-732
34. Dayton MA, Knobloch TJ, Benjamin D: Human B cell lines express the interferon gamma gene. *Cytokine* 1992, 4:454-460
35. Jelinek DF, Braaten JK: Role of IL-12 in human B lymphocyte proliferation and differentiation. *J Immunol* 1995, 154:1606-1613

36. Metzger DW, Vogel LA, Van Cleave VH, Lester TL, Buchanan JM: The effects of IL12 on B-cell subset function. *Res Immunol* 1995, 146:499-505
37. Vogel LA, Lester TL, Van Cleave VH, Metzger DW: Inhibition of murine B1 lymphocytes by interleukin-12. *Eur J Immunol* 1996, 26:219-223
38. Li L, Young D, Wolf SF, Choi YS: Interleukin-12 stimulates B cell growth by inducing IFN-gamma. *Cell Immunol* 1996, 168:133-140
39. Trinchieri G: Interleukin-12: a cytokine at the interface of inflammation and immunity. *Adv Immunol* 1998, 70:83-243
40. Airoidi I, Gri G, Marshall JD, Corcione A, Facchetti P, Guglielmino R, Trinchieri G, Pistoia V: Expression and function of IL-12 and IL-18 receptors on human tonsillar B cells. *J Immunol* 2000, 165:6880-6888
41. Zhang YP, Tzartos SJ, Wekerle H: B-T lymphocyte interactions in experimental autoimmune myasthenia gravis: antigen presentation by rat/mouse hybridoma lines secreting monoclonal antibodies against the nicotinic acetylcholine receptor. *Eur J Immunol* 1988, 18:211-218
42. Stockinger B, Zal T, Zal A, Gray D: B cells solicit their own help from T cells. *J Exp Med* 1996, 183:891-899
43. Macaulay AE, DeKruyff RH, Goodnow CC, Umetsu DT: Antigen-specific B cells preferentially induce CD4+ T cells to produce IL-4. *J Immunol* 1997, 158:4171-4179
44. Sun D, Whitaker JN, Huang Z, Liu D, Coleclough C, Wekerle H, Raine CS: Myelin antigen-specific CD8+ T cells are encephalitogenic and produce severe disease in C57BL/6 mice. *J Immunol* 2001, 166:7579-7587
45. Babbe H, Roers A, Waisman A, Lassmann H, Goebels N, Hohlfeld R, Friese M, Schroder R, Deckert M, Schmidt S, Ravid R, Rajewsky K: Clonal expansions of CD8(+) T

cells dominate the T cell infiltrate in active multiple sclerosis lesions as shown by micromanipulation and single cell polymerase chain reaction. *J Exp Med* 2000, 192:393-404

46. Weinshenker BG, O'Brien PC, Petterson TM, Noseworthy JH, Lucchinetti CF, Dodick DW, Pineda AA, Stevens LN, Rodriguez M: A randomized trial of plasma exchange in acute central nervous system inflammatory demyelinating disease. *Ann Neurol* 1999, 46:878-886

47. Kieseier BC, Hartung HP: Current disease-modifying therapies in multiple sclerosis. *Semin Neurol* 2003, 23:133-146

Figure Legends

Figure 1. Increased severity of EAE in CD19^{-/-} mice. CD19^{-/-} and wild type mice (ten per group) were immunized with MOG peptide in CFA and intravenously injected with pertussis toxin. Mice were scored for the severity of EAE using the scale described in Materials and Methods. The EAE score is shown as mean ± SEM. * p<0.05.

Figure 2. CD19^{-/-} mice had higher pathological severity scores of EAE. Spinal cords were harvested from CD19^{-/-} and wild type mice (five per group) 28 days after immunization. A representative section from each group showing lymphocyte infiltration stained by H&E (A), demyelination stained by Luxol Fast Blue (B), immunohistochemistry for CD4⁺ T cells (C) and CD8⁺ T cells (D), and the mean pathologic score of demyelination and infiltration of each group (E). Original magnifications: x200. Arrows point to focus of demyelination. Data are the mean ± SEM. * p<0.05, † p<0.005.

Figure 3. CD19 loss attenuates anti-MOG Ig production. CD19^{-/-} and wild type mice were immunized with MOG peptide in CFA. Sera (five per group) were collected on day 14 and 28, IgM (A) and IgG (B) anti-MOG Ab levels were measured by ELISA. The data are presented by the mean value of three separate measurements of each sample. Controls (n = 12) were wild type mice immunized with CFA alone.

Figure 4. The inflamed CNS tissue in CD19^{-/-} mice displays a Th1 biased cytokine production. RNA was isolated from PBS-perfused spinal cords in CD19^{-/-} and wild type mice (five per group) 28 days after immunization. The mRNA levels of IFN- γ , IL-12p40, TNF- α , IL-6 and IL-10 were analyzed by real-time RT-PCR, and normalized with internal control

GAPDH. Data are shown as mean \pm SEM. * $p < 0.05$. Mononuclear cells were isolated from pooled CNS tissue in CD19^{-/-} and wild type mice (three per group) 28 days after immunization by Percoll gradient centrifugation and incubation with PMA and ionomycin. The cells were stained with anti-CD4 and anti-CD8 \square Abs. After permeabilization, cells were stained with anti-IFN- γ Ab. Percentages of IFN- γ ⁺ cells are shown in the *upper right quadrants*. These data are representative of three independent experiments.

Figure 5. Production of high IFN- γ and low IL-10 by splenic B cells in CD19^{-/-} mice with EAE. Splenic B cells were purified from CD19^{-/-} and wild type mice (five per group) 28 days after immunization. Purified splenic B cells were incubated *in vitro* in media alone (med) or MOG peptide, anti-CD40, or both. IL-10 (A) and IFN- γ (B) accumulation in the culture medium was measured by ELISA. Data are the mean \pm SEM. * $p < 0.05$. For intracellular IL-10 (C) and IFN- γ (D) staining, purified splenic B cells were stimulated with MOG peptide and anti-CD40 mAb for 72 h, and then restimulated with PMA and ionomycin for 12 h. Intracellular cytokine staining was done using anti-B220 Ab to identify B lineage cells. Percentages of IL-10⁺ and IFN- γ ⁺ cells are shown in the *upper right quadrants*. These data are representative of three independent experiments.

Figure 6. The increased severity of EAE in CD19^{-/-} mice does not depend on the loss of IL-10 production from B cells. (A) Wild type mice were immunized with MOG peptide to induce EAE. Splenocytes were harvested 28 days after immunization. Then MOG-primed splenic B cells were purified (>95% B220⁺), and wild type B cells (10^7 cells) were transferred intravenously into CD19^{-/-} mice. One day later, the recipient mice were immunized with MOG peptide in CFA to induce EAE. The other groups, CD19^{-/-} and wild type mice, did not

receive any cells. (B) MOG-primed splenic CD19^{-/-} B cells were transferred intravenously into wild type mice, followed by immunization with MOG peptide in CFA. Mice were scored for the severity of EAE as in Figure 1.

Table 1. Infiltrating cell profile in the inflamed CNS with CD19^{-/-} and wild type mice

| Cell number/transverse section | | | | |
|--------------------------------|------------|-------------------------|-------------------------|--------------------------|
| | Macrophage | CD4 ⁺ T cell | CD8 ⁺ T cell | Total infiltrating cells |
| CD19 ^{-/-} | 51.2 ± 8.5 | 39.8 ± 10.7 | 28.0 ± 4.2† | 119.5 ± 20.8* |
| Wild type | 30.3 ± 8.4 | 29.8 ± 8.4 | 8.8 ± 2.4 | 69.0 ± 5.6 |

| Percentage of cells | | | | |
|---------------------|-------------|-------------------------|-------------------------|---------------|
| | Macrophage | CD4 ⁺ T cell | CD8 ⁺ T cell | CD4/CD8 ratio |
| CD19 ^{-/-} | 44.6 ± 3.8 | 31.3 ± 2.8 | 24.3 ± 2.9* | 1.4 ± 0.5* |
| Wild type | 43.8 ± 13.0 | 43.3 ± 11.9 | 13.0 ± 3.6 | 3.3 ± 1.5 |

Values represent the numbers or percentages of infiltrating cells in the CNS with EAE or the CD4/8 ratio. Data are the mean ± SEM. *, The numbers or percentages of cells or the CD4/8 ratio was significantly different from that of wild type mice, p<0.05; †, p<0.005. n = 5/group.

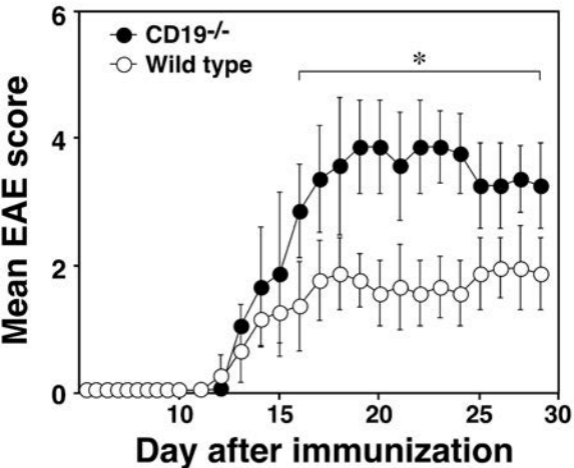


Figure1
Matsushita T, et al

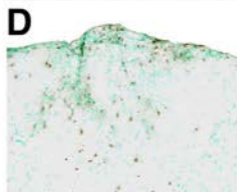
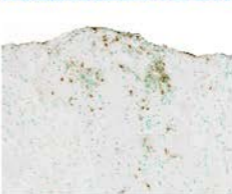
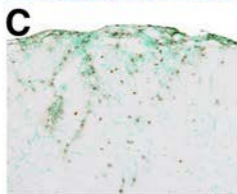
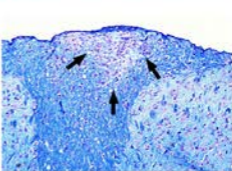
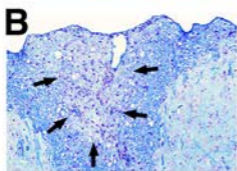
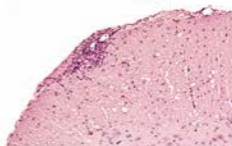
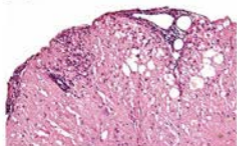
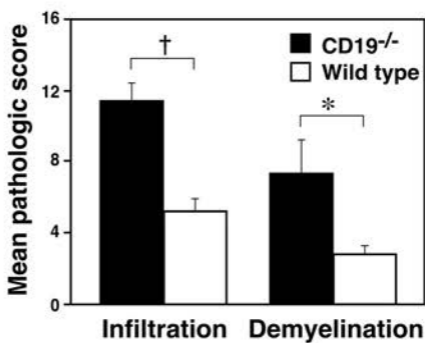
A CD19^{-/-}**Wild type****E**

Figure 2
Matsushita T, et al

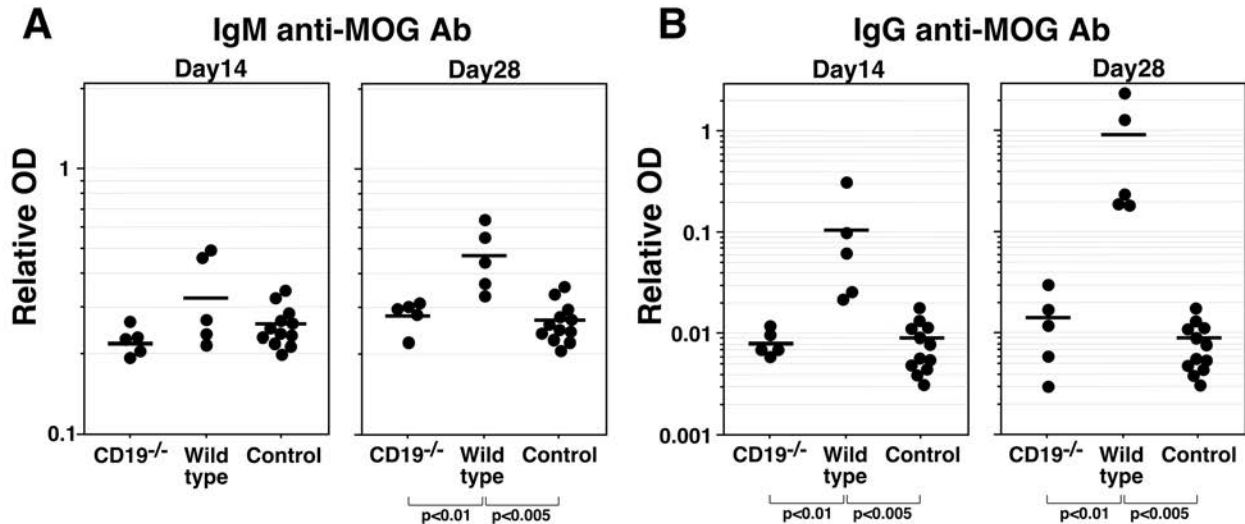


Figure3
Matsushita T, et al

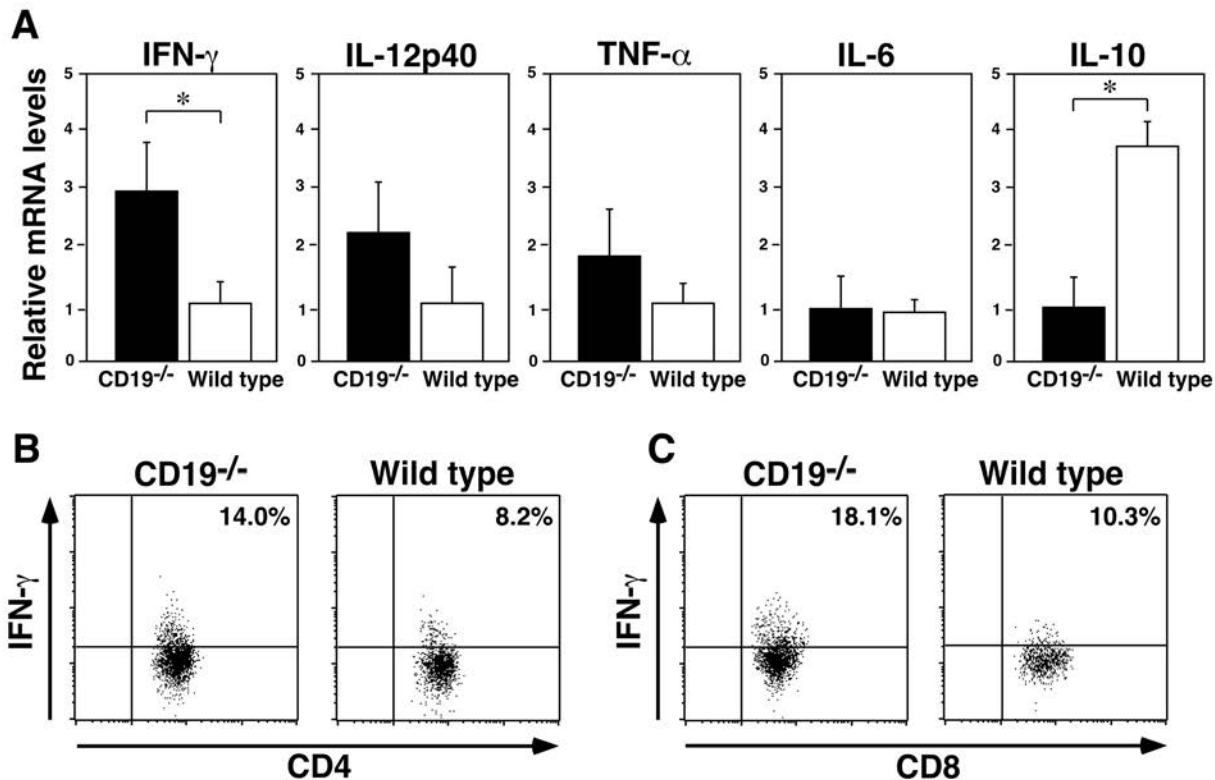


Figure 4
Matsushita T, et al

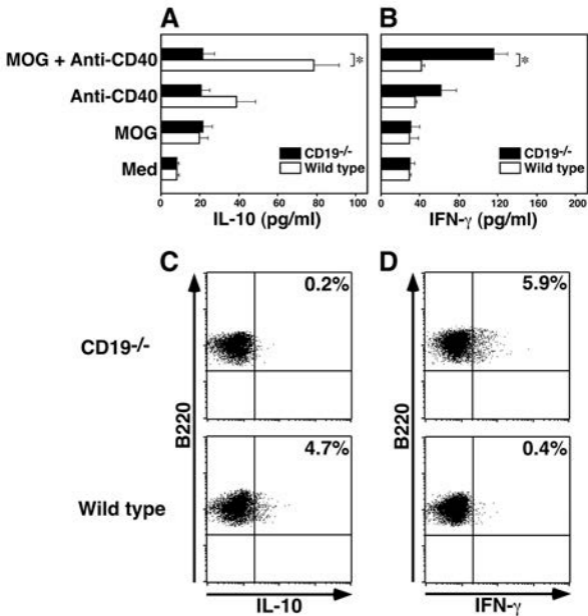


Figure5
Matsushita T, et al

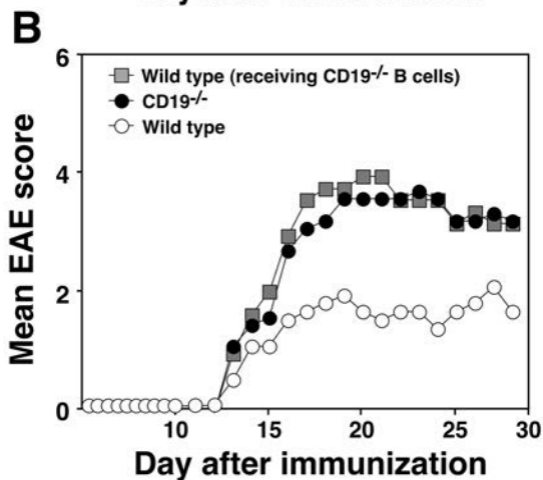
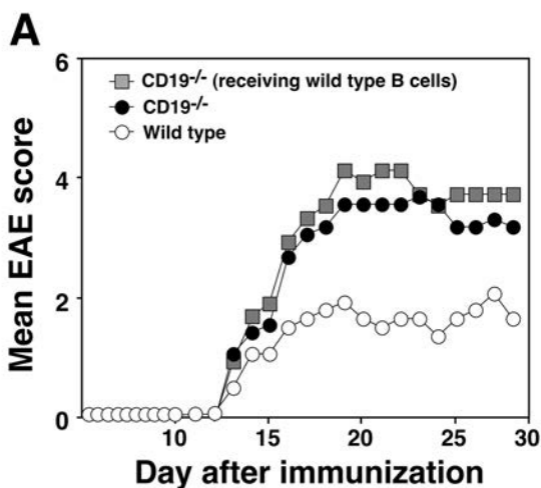


Figure6
 Matsushita T, et al